



**HAL**  
open science

## Improving the variance in Monte Carlo criticality calculations with adaptative multilevel splitting

Kévin Fröhlicher, Eric Dumonteil, Loic Thulliez, Julien Taforeau, Mariya Brovchenko

► **To cite this version:**

Kévin Fröhlicher, Eric Dumonteil, Loic Thulliez, Julien Taforeau, Mariya Brovchenko. Improving the variance in Monte Carlo criticality calculations with adaptative multilevel splitting. PHYSOR 2022 - International Conference on the Physics of Reactors, American Nuclear Society (ANS), May 2022, Pittsburgh, United States. irsn-03948886

**HAL Id: irsn-03948886**

<https://irsn.hal.science/irsn-03948886v1>

Submitted on 20 Jan 2023

**HAL** is a multi-disciplinary open access archive for the deposit and dissemination of scientific research documents, whether they are published or not. The documents may come from teaching and research institutions in France or abroad, or from public or private research centers.

L'archive ouverte pluridisciplinaire **HAL**, est destinée au dépôt et à la diffusion de documents scientifiques de niveau recherche, publiés ou non, émanant des établissements d'enseignement et de recherche français ou étrangers, des laboratoires publics ou privés.

Copyright

## **IMPROVING THE VARIANCE IN MONTE CARLO CRITICALITY CALCULATIONS WITH ADAPTATIVE MULTILEVEL SPLITTING**

**Kévin Fröhlicher<sup>1\*</sup>, Eric Dumonteil<sup>2</sup>, Loïc Thulliez<sup>2</sup>,  
Julien Taforeau<sup>1</sup> and Mariya Brovchenko<sup>1</sup>**

<sup>1</sup>Institut de Radioprotection et de Sûreté Nucléaire (IRSN)  
31 Avenue de la Division Leclerc, 92260, Fontenay-aux-Roses, France

<sup>2</sup>IRFU, CEA, Université Paris-Saclay, 91191 Gif-sur-Yvette, France

kevin.frohlicher@irsn.fr, eric.dumonteil@cea.fr, loic.thulliez@cea.fr,  
julien.taforeau@irsn.fr, mariya.brovchenko@irsn.fr

### **ABSTRACT**

This paper proposes a new iterative algorithm for Monte Carlo criticality calculations based on the Adaptative Multilevel Splitting (AMS) algorithm initially developed as a variance reduction technique. The objective is to modify the AMS and use it in place of the standard Power Iteration technique, aiming at reducing the variance, the bias, the spatial and cycle-to-cycle correlations. As a first step towards proof of concept, the method has been tested on one-dimensional homogeneous rods of different sizes, in a mono-energetic framework. The preliminary results presented here suggest that the method could provide promising improvements regarding cycle-to-cycle and spatial correlations, and thus reducing clustering. The AMS combined with branchless collision allowed for an increase in the Figure of Merit by a factor 63 for the  $k_{eff}$ , and by three order of magnitude on average for the spatial flux (from 4 to  $10^5$ ) on a 80 cm rod.

**KEYWORDS:** Monte Carlo,  $k$ -eigenvalue, correlations, clustering, Adaptative Multilevel Splitting

### **1. INTRODUCTION**

Since the beginning of simulations in the nuclear field, Monte Carlo methods have been used to address neutron transport problems with fairly good fidelity regarding the transport physics. Among these problems, the fixed-source calculation, and the so-called  $k$ -eigenvalue calculation (also called criticality calculation) are the most used when it comes to nuclear reactor applications. Concerning the former, variance reduction techniques have been widely used to improve the performances of those simulations [1,2]. As for the later, attempts have been made to accelerate their convergence [3,4] and apply variance reduction methods on the effective multiplication factor ( $k_{eff}$ ) estimate, but sometimes with limited success regarding variance reduction [5].

To solve  $k$ -eigenvalue problems with Monte Carlo methods, the classical approach is to use an iterative algorithm called the Power Iteration (PI) [6]. In this algorithm, an iteration consists in modelling the transport of neutrons over one generation (from their birth until their death by leakage or absorption),

---

\*Corresponding author.

and save the neutrons produced by fission for that generation/cycle. A renormalization of the neutron population is then done by sampling the sources for the next iteration from the neutrons saved during the current iteration (born by fission). The process is repeated until spatial convergence of the sources has been reached. These so-called inactive cycles are then discarded, and more iterations are done (the active cycles) to be used to compute an average of the scores.

Ueki and Brown, as well as Dumonteil et al. [7,8] have shed the light on the fact that strong spatial and generational correlations can arise in criticality calculations. In fact, successive cycles are correlated in the Power Iteration, because of the way source neutrons are sampled in each cycle [6]. Such correlations can cause some serious challenges for the estimation of eigenvalue ( $k_{eff}$ ) and eigenvector (the spatial distribution of the flux, and so, the derived quantities) [9,10]. While methods have been studied to reduce the effects of those correlations (hence, reducing the "true" variance) [11], they do not allow a reduction of the observed variance. The following work aims at addressing the issue of variance reduction in criticality calculations and correlation issues through a new iterative algorithm in criticality, derived from previous work on Adaptive Multilevel Splitting for fixed source problems [2].

## 2. THE ADAPTATIVE MULTILEVEL SPLITTING

The Adaptive Multilevel Splitting (AMS) is a variance reduction technique inherited from the field of applied mathematics [12,13], its original purpose is to help the computation of rare events in the case of Markov chains. It has been adapted to particle transport for reactor physics [2], initially for attenuation and shielding problems in non-multiplying medium. The following descriptions is partly taken from previous work found in literature [14], and concerns the algorithm intended to fixed source problems in multiplying media.

### 2.1. The Method

The idea behind the AMS algorithm for particle transport is to push the initial particles towards a detector. During the first iteration,  $N$  particles are tracked until their death and will represent  $N$  different tracks that will be followed during the next iterations. For multiplying media, each time a branching reaction occurs, a new branch is added to the track.

At the end of an iteration, tracks are ranked according to their importance, which is defined by the maximum importance reached during the simulation by the branches inside that track. The importance function itself must be provided by the user. Then, a splitting level is defined as the  $K$ -th worst track's importance, and all the  $K_i$  tracks having an importance lower or equal to that level are discarded.  $K_i$  tracks are then chosen randomly among the  $N - K_i$  surviving ones and split at their first point whose importance is higher than the splitting level, so that the system again contains  $N$  tracks. At this point, a new iteration starts. The whole process is repeated until at least  $N - K + 1$  tracks have reached the detector.

To keep an unbiased result, the final score is then weighted by the renormalizing factor computed during the last iteration, defined by

$$\alpha_i = \prod_{j=1}^i \left(1 - \frac{K_j}{N}\right) \quad (1)$$

where  $K_j$  is the effective number of tracks re-sampled during iteration  $j$ .

For multiplying systems, when surviving tracks are selected for splitting, it is necessary to consider all the branches of that track above the splitting level and copy them into the new track.

The method has shown good results for attenuation problems (comparable to those of exponential transform, the method could even compute a flux when the analog method could not, due to a lack of particles

[14]). It has the interesting feature to be simple of use since only two parameters have to be set by the user (except for the importance function), the total number of tracks  $N$  and the number of tracks re-sampled at each iteration  $K$ . Concerning the importance function, it is only used to rank particles between them. This means that simple importance maps (e.g. distance to the detector) can be used to achieve an already interesting variance reduction.

More details can be found in the original publications (for particle transport in fixed source problems) [2,14].

## 2.2. Adaptation to Criticality Calculations

In criticality calculations, the  $k_{eff}$  and the flux distribution (and derived quantities) are computed using the Power Iteration algorithm. In this algorithm, the neutron population is normalized at each iteration/cycle in order to follow the system across numerous successive generations, without seeing the system die or diverge in population.

To do so with the AMS, we follow the particles, not just in the phase space but also in time. Our idea is to push the neutrons towards a "time-detector" (here a target generation), and compute the score over intermediate generations.

Pushing particles toward the target generation requires a simple importance function  $\xi(g, \mathbf{r})$  defined here as

$$\xi(g, \mathbf{r}) = g + f(\mathbf{r}) \quad (2)$$

where  $g$  is the generation of the particle and  $f$  a function whose image lies in the interval  $[0, 1[$ . Here  $f(\mathbf{r})$  is only set to discriminate particles inside the same generation and avoid a neutrons accretion in one generation, which could lead to an early stop of the iterations. In this paper,  $f(\mathbf{r}) = \frac{1}{1 + |x|}$  was chosen, which allows to favor particles at the center of the geometry (i.e. those with the less chances to leak outside the system) for a given generation.

In multiplying media, following neutrons continuously in time implies dealing with a potentially diverging number of neutrons [15]. The AMS described in the previous section is only adapted for sub-critical systems. Hence, to avoid the number of AMS branches to diverge, particles were transported using the improved branchless method [16], to model critical and supercritical configurations. This method replaces branching and death due to fission and capture by a neutron's weight variation, so that exactly one neutron is emitted at each collision. Therefore, the initial algorithm becomes the following. The first iteration consists in sampling  $N$  neutrons using a uniform distribution. They are then transported across several generations until all their progeny has left the system (by leakage). Then  $K$  tracks are selected for re-sampling, and transported during the next iteration until they become extinct. The iterative process is carried out until  $N - K + 1$  tracks have reached the target generation. The scores are then computed for each scoring volume (i.e. each successive generation). To compute the  $k_{eff}$  at generation  $g$  following

$$k_{eff}^{(g)} = \frac{\phi_g}{\phi_{g-1}} \quad (3)$$

with  $\phi_g$  the total flux estimated at generation  $g$ .

For the shape of the flux, its integral over space is normalized to one in each generation since we are only interested in its spatial distribution. Doing this, we can average it over the successive generations as it is done in the Power Iteration algorithm.

It is interesting to note that in this framework, particles are followed through time, and the splitting (i.e. the re-sampling of deleted tracks) can happen not only at production sites, but any type of collision point. Therefore, this algorithm show great similarities with an  $\alpha$ -eigenvalue algorithm [17].

### 3. APPLICATION TO HOMOGENEOUS 1D RODS WITH LEAKAGE

The AMS for criticality was first tested on simple cases for a proof of concept. The calculations were performed with a toy-model Monte Carlo code developed at the Institute for Radiological Protection and Nuclear Safety (IRSN). It only deals with mono-energetic particles, so no spectral effects were considered for this proof of concept.

The geometry is a one-dimensional homogeneous fuel rod with leakage (void boundary condition) at each end of the rods. Two configurations were modeled. Two rods, 20 cm and 80 cm, were simulated to evaluate the method regarding correlations on systems of different sizes. The physical properties of the two cases are shown in Table I. The systems were taken arbitrarily close to critical state (if energy had been taken into account, it would have been necessary to be close to  $k_{eff} = 1$  since spectrum effects would have biased the Power Iteration's results, compared to a dynamic or  $\alpha$ -focused algorithm [17]).

As for the simulation parameters, all cases/methods were modeled/used with 1000 neutrons per generation (for the AMS with branchless collision, this corresponds to 1000 initial tracks), over 1000 successive generations in 100 independent runs.

**Table I: Physical properties for homogeneous 1D rods**

Mean number of fission neutrons ( $\bar{\nu}$ )	2.325
Neutron speed ( $v$ )	$2.2 \times 10^4 \text{ cm.s}^{-1}$
Macroscopic cross sections	
Fission ( $\Sigma_f$ )	$0.250 \text{ cm}^{-1}$
Absorption ( $\Sigma_a$ )	$0.575 \text{ cm}^{-1}$
Scattering ( $\Sigma_s$ )	$0.425 \text{ cm}^{-1}$
Total ( $\Sigma_{tot}$ )	$1.00 \text{ cm}^{-1}$

#### 3.1. Study of the Convergence

To compare the convergence speed of the two algorithms, the Shannon entropy of the fission sites is monitored over generations. Here the Shannon entropy for the fission sites is computed over 100 bins, as follow

$$H = - \sum_{j=1}^{100} p_j \log_2(p_j) \quad (4)$$

where  $p_j$  is the number of fissions in bin  $j$  over the total number of fissions in the whole geometry, with  $p_j \log_2(p_j)$  set to 0 if  $p_j = 0$ .

The computed entropy is shown on Figure 1. No significant differences between the Power Iteration (PI) and the AMS are observed in the case of a 20 cm rod. For the 80 cm rod, the AMS seems to converge faster and to have a more stable entropy than the Power Iteration. For loosely coupled systems, the AMS could provide an acceleration of the convergence regarding the Shannon entropy criterion, compared to the Power Iteration.

In the next section, the results obtained after convergence for the  $k_{eff}$ , the flux and the correlations are presented. To compare the two methods with the same number of particles, both algorithm were supposed to have converged after the same number of generations  $g_{conv}$ , based on Shannon entropy observation

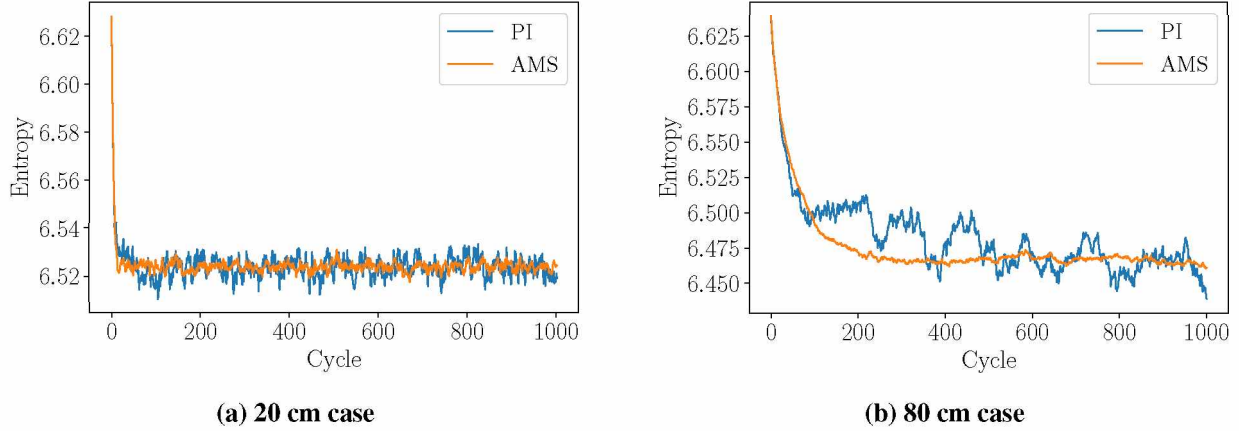


Figure 1: Comparison of Shannon entropy for PI and AMS

(Figure 1, 20 for the 20 cm rod and 500 for the 80 cm rod), even if the AMS seems to converge faster for the 80 cm rod (around generation 200 according to Figure 1b).

### 3.2. Numerical Results on Effective Multiplication Factor, Flux and Correlations

#### 3.2.1. Effective multiplication factor

The  $k_{eff}$  was averaged over  $(1000 - g_{conv}) \times N_{simu}$  estimations for both methods, where  $(1000 - g_{conv})$  is the number of successive generations and  $N_{simu}$  is the number of independent runs.  $g_{conv}$  was set regarding the Shannon entropy convergence of the Power Iteration in each case. The Figure of Merit (FoM) was computed to assess the efficiency of the two algorithms, it is generally defined as

$$FoM = \frac{1}{\sigma^2 T} \quad (5)$$

where  $\sigma$  is the standard deviation of the mean and  $T$  the computation time. Here, the results are presented as FoM ratios, so that for a method

$$FoM = \frac{FoM(method)}{FoM(PI)}. \quad (6)$$

Table II shows that the AMS produces less scattered results around the mean as the  $3\sigma$  uncertainty is lower than for the Power Iteration, as seen on the 99.7% confidence interval in Table II, which results in an increased FoM for the AMS, despite higher computational costs due to the ranking and resampling of tracks. The effect is even stronger for the 80 cm rod.

#### 3.2.2. Spatial flux

The flux spatial shape  $\phi(x)$  was also averaged in the same way as the  $k_{eff}$ . The resulting profile is represented on Figure 2. While AMS and Power Iteration are in good agreement for the 20 cm case (Figure 2a), discrepancies not covered by a  $\pm 3\sigma$  interval appear between the two methods for the 80 cm rod. Given that the system is symmetric, the 80 cm rod's spatial flux was represented as a function of the distance to  $x = 0$  on Figure 3, to check for asymmetries in both calculations. It appears that the Power Iteration produces asymmetrical results with  $3\sigma$  error bars that are not coherent with the discrepancies between  $\phi(x)$  and  $\phi(-x)$  (Figure 3a). This has been observed previously by Dumonteil et al. [18,9], and is due to particle clustering. Whereas for the AMS, the results for  $x < 0$  and  $x > 0$  are in good agreement. It seems that the

**Table II: Results on  $k_{eff}$  estimation (without accounting for correlations).**

Case	Method	$g_{conv}$	$\overline{k_{eff}}$	99.7% C.I.	FoM
20 cm	PI	20	0.97604	[0.97567; 0.97640]	1
	AMS		0.97612	[0.97606; 0.97618]	4.80
80 cm	PI	500	1.00779	[1.00728; 1.00830]	1
	AMS		1.00828	[1.00825; 1.00830]	$3.86 \times 10^1$

AMS is less prone to clustering than the Power Iteration. To assess for the clustering, the effects of the two algorithms on spatial and cycle-to-cycle correlations are presented below for the 80 cm rod.

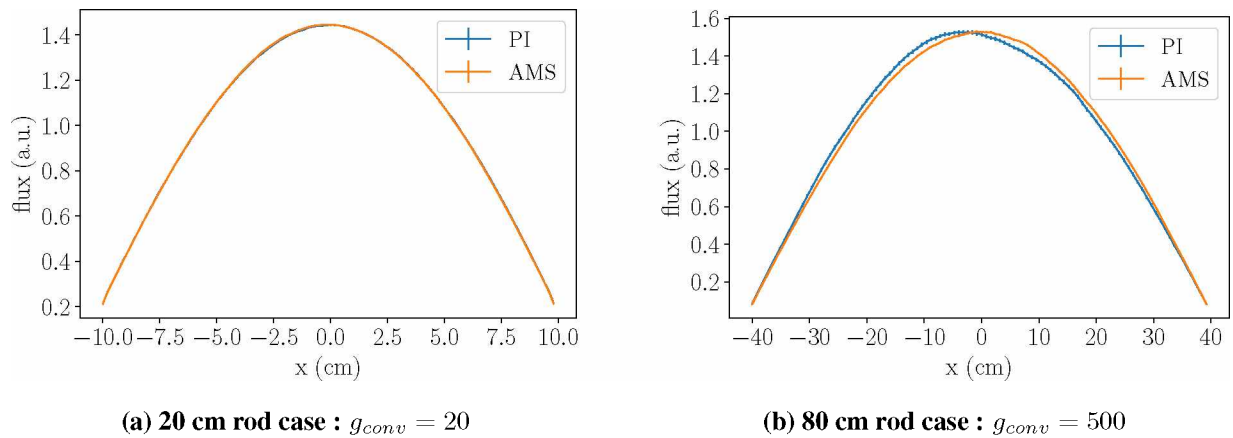


**Figure 2: Mean spatial flux  $\pm 3\sigma$  after convergence ( $g > g_{conv}$ ) for Power Iteration (PI) and AMS**

### 3.2.3. Correlations

To carry out a diagnostic of the clustering, spatial and cycle-to-cycle correlations were computed. The spatial correlations are defined as correlation factors between pairs of spatial bins by

$$\rho(x_i, x_j) = \frac{Cov(\phi(x_i), \phi(x_j))}{\sigma_{\phi(x_i)}\sigma_{\phi(x_j)}} \quad (7)$$

where  $\rho(x_i, x_j)$  is the correlation factor between bin  $i$  and bin  $j$ ,  $Cov$  refers to the covariance,  $\phi(x_i)$  is the flux in bin  $i$  and  $\sigma_{\phi(x_i)}$  is the associated standard deviation. Those quantities were computed at an arbitrary cycle (here 900) over the 100 independent runs. Figure 4 displays the spatial correlation matrix for the 80 cm rod. It can be seen that the maximum length for spatial correlation is 20 cm with the Power Iteration, and almost zero with the AMS, which means that clusters are more likely to appear with the Power Iteration than with the AMS.

For a better understanding of the clusters in this case, fission sites are plotted on Figure 5 for the Power Iteration and the AMS. It shows that clusters of fission sites are more present for the Power Iteration than for the AMS.

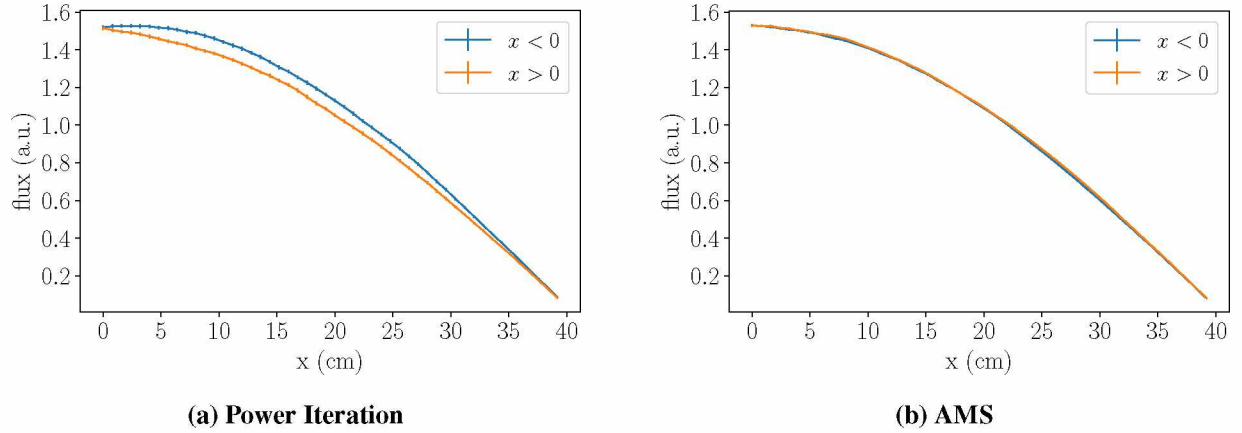


**Figure 3: Mean spatial flux  $\pm 3\sigma$  after convergence ( $g > 500$ ) for the 80 cm rod for Power Iteration (PI) and AMS**

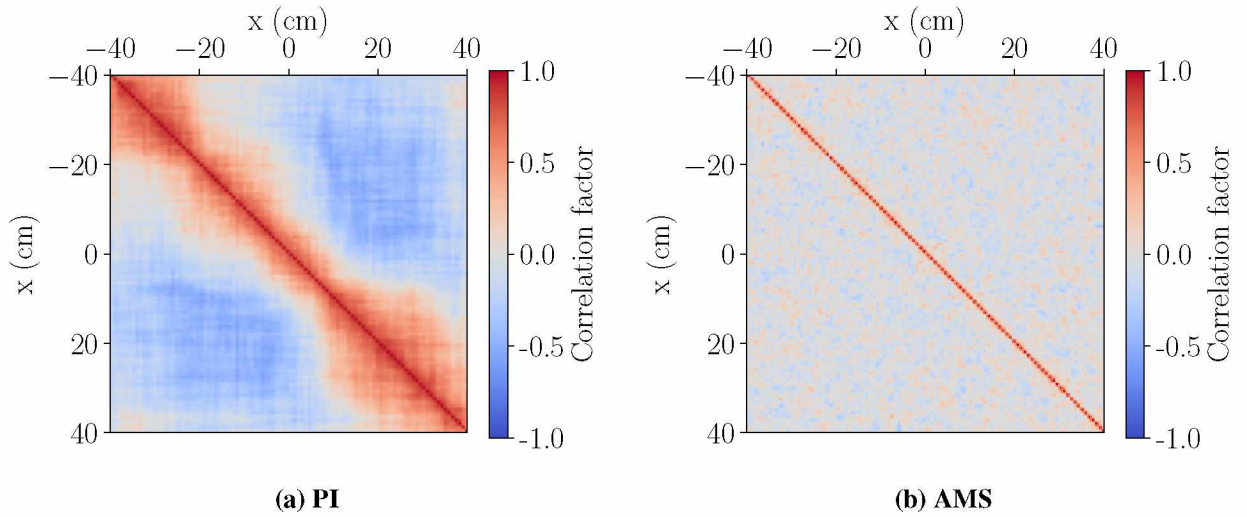


**Figure 4: Spatial correlations for the 80 cm rod at cycle 900 for Power Iteration (PI) and AMS**

In the Power Iteration algorithm, cycle-to-cycle correlations arise due to the fact that produced fission neutrons are combed between each cycle [17], i.e. the source for cycle  $i$  is sampled among fission neutrons of cycle  $i - 1$  [6]. Those cycle-to-cycle correlations were computed as follow

$$\rho_k(x) = \frac{Cov(\phi_{g_0}(x), \phi_{g_0+k}(x))}{\sigma_{\phi_{g_0}(x)}\sigma_{\phi_{g_0+k}(x)}} \quad (8)$$

where  $\rho_k(x)$  is the Pearson correlation coefficient for the flux in  $x$  between generation  $g_0$  and  $g_0 + k$ ,  $\phi_{g_0}(x)$  is the flux at  $x$  in generation  $g_0$  and  $\sigma_{\phi_{g_0}(x)}$  its standard deviation. The evolution of the correlation factor is represented on Figure 6a for the 80 cm rod, for one spatial bin located around  $x = -17$  cm, for  $k$  from 0 to  $g_{max} - g_0$ , where  $g_0 = 500$ . It shows that the correlation factor decrease more rapidly for the AMS than the Power Iteration (PI). To assess for the attenuation speed of cycle-to-cycle correlations over all  $x$ , the correlation cut-off, arbitrarily defined as the minimum number of generation  $k$  for which  $\rho_k(x) < 0.1$ ,

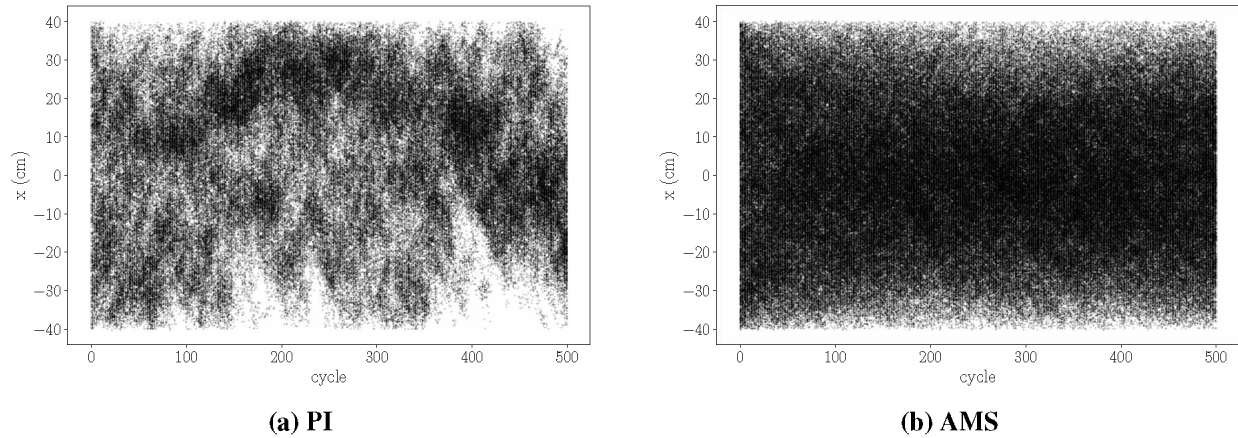
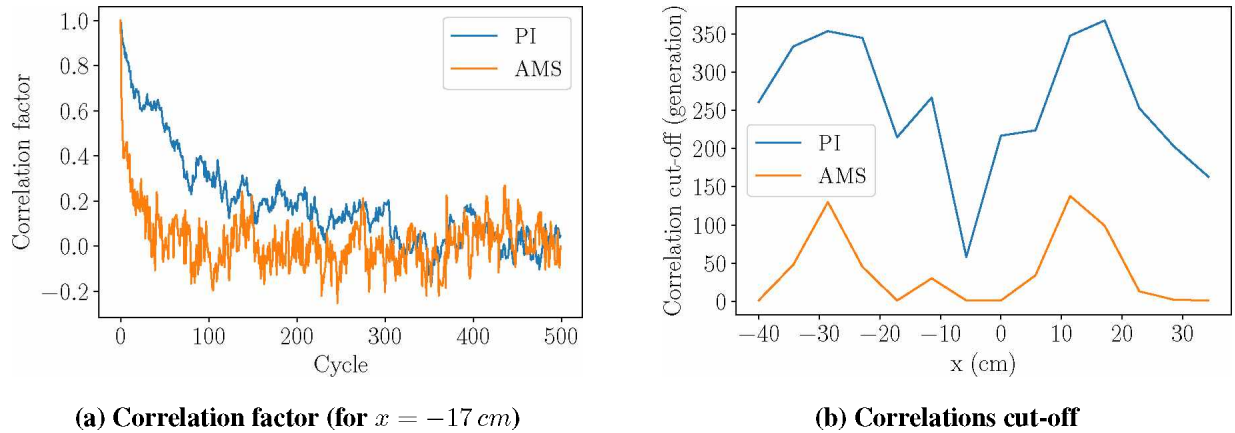


**Figure 5: Fission sites over the first 500 cycles for one of the 100 independent runs, in the case of the 80 cm rod for Power Iteration (PI) and AMS**

was computed. It is displayed on Figure 6b. This Figure shows that generational correlations seem to last much longer in the Power Iteration than in the AMS, regardless of  $x$ . For both cases, a minima is observed on the center of the geometry, which matches the minima of the module of the flux first harmonic [18]. The correlation cut-off also has local minimums on the sides due to the fact that the spatial bins on the edges only have one neighbor.



**(a) Correlation factor (for  $x = -17$  cm)**

**(b) Correlations cut-off**

**Figure 6: Cycle-to-cycle correlations for the 80 cm rod for Power Iteration (PI) and AMS**

Multiple factors may be at the origin of those effects on correlations. First, in criticality, AMS method uses the branchless collision (see section 2.2). By doing this, the extinction of families is lessened and this could lower the chances to see clusters appear [19]. In addition, only a portion  $K_j/N$  of the tracks are splitted at AMS iteration  $j$ , and since the neutron histories are run until their death, multiple generations can be travelled across until it is necessary to re-sample. For this reason, AMS iterations show similarities with the superhistory method [11].

Finally, the real variances were computed considering the cycle-to-cycle correlations. The FoM calculated with this variance are presented in Table III. The AMS simulation shows far better FoM for the estimations of the  $k_{eff}$  and the spatial flux. For the 20 cm rod, one can observe that our implementation of the AMS

deteriorates the flux FoM at some locations ( $Min(FoM) < 1$  for the AMS). This is probably because correlations are less important on small systems (this is why no clustering is observed on Figure 2a), so our algorithm might not bring improvements everywhere despite its higher computational cost.

**Table III: Results accounting for correlations.  $g_{conv}$  is set regarding the Shannon entropy convergence of each case. Average values are computed for  $g > g_{conv}$ .**

Case	Method	$g_{conv}$	$k_{eff}$			Spatial Flux		
			$\overline{k_{eff}}$	$\sigma(k_{eff})$	FoM	$Min(FoM)$	$Max(FoM)$	$\overline{FoM}$
20 cm	PI	20	0.97604	$1.22 \times 10^{-4}$	1	1	1	1
	AMS		0.97612	$1.96 \times 10^{-5}$	4.80	$2.40 \times 10^{-4}$	$1.08 \times 10^3$	$1.36 \times 10^1$
80 cm	PI	500	1.00779	$1.70 \times 10^{-4}$	1	1	1	1
	AMS	200	1.00828	$6.10 \times 10^{-6}$	$6.29 \times 10^1$	4.37	$9.49 \times 10^4$	$1.81 \times 10^3$

#### 4. CONCLUSIONS

To summarize, this work presents how the Adaptive Multilevel Splitting was modified into a new algorithm aiming at reducing the variance, and unwanted correlations, for the resolution of  $k$ -eigenvalue problems. The results compiled here show promising results regarding the initial goal since the AMS seems to bring a way to ensure faster convergence and less neutron clustering on larger systems than the classical Power Iteration. In the end, an increase of a factor 63 has been observed for the FoM on the  $k_{eff}$  estimation, and of three orders of magnitude on average for the flux in the 80 cm rod.

However, these encouraging results should be considered with care since the study is limited to one-dimensional homogeneous and mono-energetic systems, and call for more extensive studies to be conducted. On-going developments should allow a deeper analysis of the method on more complex systems. Besides, the results might be closer to the solution of an  $\alpha$ -eigenvalue problem due to the way particles are handled in time in this method. This should be a matter for further study, especially since spectral effects have a non-negligible impact on the  $k_{eff}$  and the flux estimations between  $\alpha$  and  $k$  modes when ones move away from criticality [17].

#### REFERENCES

- [1] J. S. Hendricks and T. E. Booth. "MCNP variance reduction overview." In *Monte-Carlo Methods and Applications in Neutronics, Photonics and Statistical Physics*, pp. 83–92. Springer Berlin Heidelberg (1985).
- [2] H. Louvin, E. Dumonteil, T. Lelièvre, M. Rousset, and C. M. Diop. "Adaptive multilevel splitting for Monte Carlo particle transport." In *EPJ Web of Conferences*, volume 153, p. 06006. EDP Sciences (2017).
- [3] T. J. Urbatsch. *Iterative acceleration methods for Monte Carlo and deterministic criticality calculations*. Ph.D. thesis, University of Michigan (1995).
- [4] A. Jinaphanh, J. Miss, Y. Richet, N. Martin, and A. Hébert. "Exploring the use of a deterministic adjoint flux calculation in criticality monte carlo simulations." *Proceedings of M&C 2011* (2011).
- [5] A. Jinaphanh. *Etudes de la convergence d'un calcul Monte Carlo de criticité: utilisation d'un calcul déterministe et détection automatisée du transitoire*. Ph.D. thesis, Université de Grenoble (2012).

- [6] I. Lux and L. Koblinger. *Monte Carlo Particle Transport Methods*. CRC-Press (1991).
- [7] T. Ueki, F. B. Brown, D. K. Parsons, and D. E. Kornreich. “Autocorrelation and dominance ratio in Monte Carlo criticality calculations.” *Nuclear science and engineering*, **volume 145**(3), pp. 279–290 (2003).
- [8] E. Dumonteil, F. Malvagi, A. Zoia, A. Mazzolo, D. Artusio, C. Dieudonné, and C. De Mulatier. “Particle clustering in Monte Carlo criticality simulations.” *Annals of Nuclear Energy*, **volume 63**, pp. 612–618 (2014).
- [9] E. Dumonteil, G. Bruna, F. Malvagi, A. Onillon, and Y. Richet. “Clustering and traveling waves in the Monte Carlo criticality simulation of decoupled and confined media.” *Nuclear Engineering and Technology*, **volume 49**(6), pp. 1157–1164 (2017).
- [10] P. Cosgrove, E. Shwageraus, and G. Parks. “Neutron clustering as a driver of Monte Carlo burn-up instability.” *Annals of Nuclear Energy*, **volume 137**, p. 106991 (2020).
- [11] R. Brissenden and A. Garlick. “Biases in the estimation of keff and its error by Monte Carlo methods.” *Annals of Nuclear Energy*, **volume 13**(2), pp. 63–83 (1986).
- [12] F. Cérou and A. Guyader. “Adaptive multilevel splitting for rare event analysis.” *Stochastic Analysis and Applications*, **volume 25**(2), pp. 417–443 (2007).
- [13] C.-E. Bréhier, M. Gazeau, L. Goudenège, T. Lelièvre, and M. Rousset. “Unbiasedness of some generalized adaptive multilevel splitting algorithms.” *The Annals of Applied Probability*, **volume 26**(6), pp. 3559–3601 (2016).
- [14] H. Louvin. *Development of an adaptive variance reduction technique for Monte Carlo particle transport*. Ph.D. thesis, Université Paris-Saclay (2017).
- [15] T. E. Harris et al. *The theory of branching processes*, volume 6. Springer Berlin (1963).
- [16] B. L. Sjenitzer and J. E. Hoogenboom. “Dynamic Monte Carlo method for nuclear reactor kinetics calculations.” *Nuclear Science and Engineering*, **volume 175**(1), pp. 94–107 (2013).
- [17] D. E. Cullen, C. J. Clouse, R. Procassini, and R. C. Little. “Static and dynamic criticality: are they different?” Technical report, Lawrence Livermore National Lab., Livermore, CA (US) (2003).
- [18] E. Dumonteil and F. Malvagi. “Automatic treatment of the variance estimation bias in TRIPOLI-4 criticality calculations.” In *Proceedings of the 2012 International Congress on Advances in Nuclear Power Plants - ICAPP '12*. Chicago, IL (United States) (2012).
- [19] T. M. Sutton. “Toward a more realistic analysis of neutron clustering.” *Proceedings of M&C 2021*, pp. 1555–1566 (2021).